IMPROVED ANALYTICAL PREDICTION OF BOUNDARY-LAYER INDUCED ROTOR NOISE USING CIRCUMFERENTIAL MODES

Martin STAGGAT, Antoine MOREAU,
Sébastien GUÉRIN

German Aerospace Center (DLR) e.V.
Institute of Propulsion Technology, Department for Engine Acoustics
Müller-Breslau-Straße 8, 10623 Berlin, Germany

SUMMARY

An improved theory addressing the interaction noise of a turbulent boundary layer with a rotor is presented. Compared to a prior version, central components, such as the prediction of the turbulent velocity spectra, the correlation lengths and the stream tube contraction, are modified or included to better address the strongly anisotropic character of the boundary layer turbulence. The predictions with the improved theory show a better agreement with some benchmark data with regard to the amplitude and spectral shape of the sound pressure signals.

INTRODUCTION

Modern civil aircraft are submitted to stringent regulations concerning the emission of pollutants and noise to limit their environmental impact and ensure the acceptance of growing air traffic. In the mid and long term this demand will not be satisfied by the classical tube-wing aircraft architecture, as we suppose it has already come close to its optimum design – a compromise between technology and costs. The introduction of new technologies, such as boundary layer ingesting (BLI) engines, shows a potential towards a transformation of the aircraft shape to fuel-efficient blended or hybrid wing bodies with embedded engines [1]. Beside the benefits of BLI engine concepts in terms of propulsion efficiency new concerns arise about the noise emission of such configurations resulting from the highly distorted engine inflow interacting with the fan.

The problem of broadband noise resulting from the interaction of ingested turbulence with a rotor or fan was addressed by several authors: Mani [2] was one of the first who attributed the noise emitted at the blade passing frequency (BPF) by a rotor-stator stage with a cut-off design to the ingested turbulence. The author presented a theory in the frequency domain based on the two-point velocity correlation. The rotor blades are modelled as flat plates. As inflow, homogeneous and isotropic turbulence is assumed. For a sufficiently high ratio of the turbulent length scale to the blade spacing, peaks at the BPF and its higher harmonics are predicted in the broadband noise (BBN) spectrum. By developing an analytical technique Homicz and George [3] proved that the ratio of the time taken by a rotor to complete one revolution to the time needed by one integral scale of turbulence to propagate through the rotor plane is the most important parameter affecting the occurrence and shape of the peaks. By using the theory of Amiet [4] in a modified form, Paterson

and Amiet [5] identified that a correct description of the anisotropy of the ingested turbulence is required to obtain reasonable turbulence-rotor interaction noise predictions. Based on Mani's work Kerschen and Gliebe [6] formulated a more generalised model for the prediction of turbulence rotor interaction noise. In that model, the turbulence is assumed to be anisotropic and axisymmetric (cylindrical-shaped). The authors considered the dipole and quadrupole contribution. Again, for a sufficiently high ratio of the longitudinal length scale of turbulence to the blade spacing, peaks at the BPF and its harmonics are predicted. They also showed that the peak width is inversely proportional to the longitudinal length scale of the turbulence whereas the peak amplitude is independent of this length scale. Glegg and Walker [7] presented a theory based on Glegg [8] for the prediction of noise resulting from the casing boundary layer with a rotor. They showed that modelling of the turbulent boundary layer anisotropy is necessary to predict the measured peaks with correct amplitude at the BPF and its harmonics. Concerning BBN resulting from the interaction of a turbulent boundary layer with a rotor, Glegg et al. [9] described an approach that accounts for the blade-to-blade correlation, anisotropy and inhomogeneity of the turbulence. Different forms for the needed two-point correlation function and its impact on the acoustic results were discussed by the authors. The models of the aforementioned work are formulated in the frequency domain using a description in circumferential modes. The analytical theory discussed in the present paper follows a similar approach.

As an alternative to the frequency domain approach, Stevens and Morris [10] formulated theory in the time domain using two-point correlation functions to predict the interaction noise of inhomogeneous and anisotropic turbulence with a rotor. They confirmed that the presence of turbulence contributes significantly to broadband but also tonal noise despite of the absence of a mean velocity distortion. To overcome the necessity to model two-point correlation functions in the frequency domain, Glegg et al. [11] also developed a time-domain method that directly uses two-point correlation measurements in the rotating frame.

Amongst others, the impact of stream tube contraction on ingested turbulence is addressed by Ganz [12]. He defined contraction ratios based on the velocities before and after the stream tube contraction to describe the deformation of fluid filaments. Majumdar and Peake [13] identified the longitudinal stretching of turbulence as the most relevant dynamic process and apply Rapid Distortion Theory (RDT) within their prediction method for BBN resulting from the interaction of turbulence with rotor blades. Atassi and Logue [14] used a three-dimensional linear cascade model to predict the noise from the interaction of anisotropic and axial-symmetric turbulence with a blade row. Peaks at the BPF and its higher harmonics were observed for a sufficiently large stretching of the turbulence in the mean-flow direction.

The DLR Department of Engine Acoustics is developing an analytical tool that allows the prediction of several tonal and broadband fan noise sources [15]. In an earlier publication [16] a theory based on circumferential modes in the frequency domain was presented for the prediction of BBN caused by the ingestion of a turbulent boundary layer interacting with an open rotor. This theory is able to predict peaks in the BBN spectrum at the BPF and its harmonics. The present paper aims at improving this theory. The isotropic von Kármán spectrum used priory is replaced by the anisotropic Kerschen-Gliebe spectra. The estimation of the transversal correlation length is substituted by a recently published recalibrated model [17] developed for turbulent boundary layers. By accounting for the stream tube contraction following Ganz [12], this model allows determining the longitudinal correlation length, which is used to determine the blade-to-blade correlation.

The paper is organised as follows: The analytical theory is presented in the next section and the improved components are discussed. Afterwards, the analytical model is applied to a benchmark case representing an open rotor interacting with a turbulent boundary layer. Noise predictions are compared with measurements at different operating conditions.

THEORY

Assumed phenomenology

According to the aforementioned work [2, 6-14, 16-17 and 24-28] the modelling of the anisotropic character of the turbulence and in general the deformation of the associated coherent structures during ingestion is required to accurately predict the noise generated by a rotor interacting with a turbulent boundary layer.

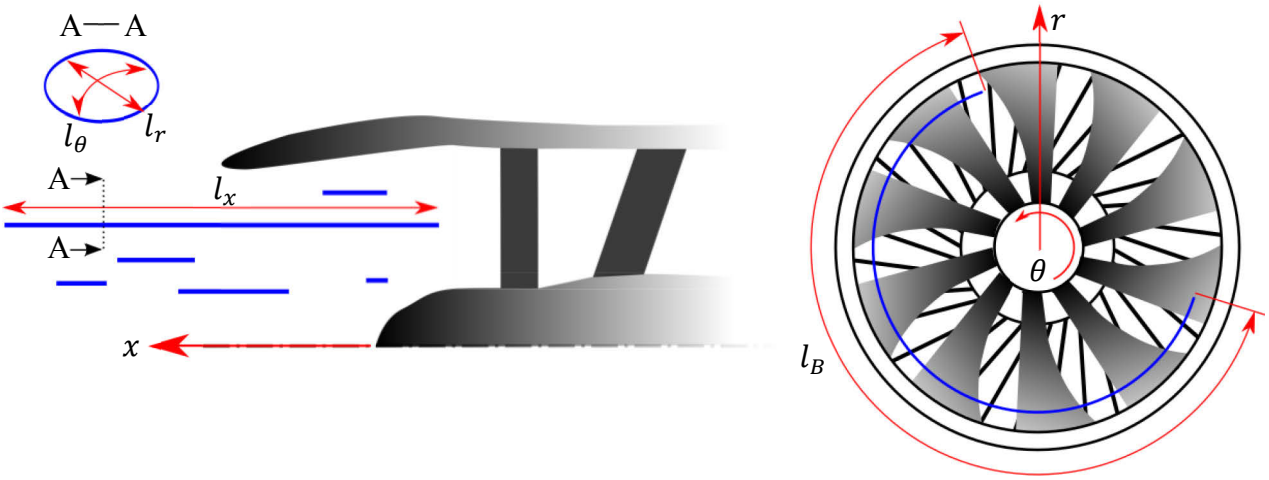

Fig.1: Illustration of assumed anisotropic and axisymmetric turbulence.
Picture taken from Staggat et al. [16]. Reproduced with permission.

Figure 1 illustrates the phenomenology of anisotropic axisymmetric turbulence used for the theory considered in the present paper. Different correlation lengths are introduced: l_x in axial direction, l_r in radial and l_θ in circumferential directions. Note that l_r and l_θ are assumed to be equal and are replaced by a single transversal correlation length l_t. The axial extent of a coherent structure may reach several hundred times its transversal extent as shown by Hanson [18]. Due to the long correlation length of a structure in axial direction, consecutive rotor blades cut the same turbulent structure. The resulting pressure variations on those blades are partly correlated. That effect is parametrised by the blade correlation length l_B in the rotating frame and can result in the excitation of interaction modes, whose circumferential orders m depend on the mode order of the incoming distortion m_0 and the rotor blade count B. Furthermore the small transversal correlation length of the incoming turbulence leads to an excitation of aerodynamic modes with high order m_0, which is required to excite the acoustic interaction modes m [16].

Aerodynamic excitation model

As proposed by Moreau [15] and Staggat et al. [16] the aerodynamic modal excitation auto-spectrum is formulated as:

$$\Phi_{uu}(f, m_0) = F(m_0, l_t, r) \cdot \frac{1}{2\pi} \int_0^{2\pi} S_{\theta\theta}(f)\, \mathrm{d}\theta, \tag{1}$$

$$\text{with } F(m_0, l_t, r) = \frac{l_t}{2\pi\, r} \exp\left(-\frac{m_0^2 l_t^2}{4\pi\, r^2}\right). \tag{2}$$

The coherence function $F(m_0, l_t, r)$ is introduced to model the actually required cross-spectrum $S_{\theta\theta'}(f)$ by an auto-spectrum $S_{\theta\theta}(f)$. This Gaussian function is assumed to be 2π-periodic in

circumferential direction θ. It depends on the transversal correlation length l_t and the radial position r. This function determines the number of aerodynamic modes m_0 involved. Note that Eq.(2) ensures conservation of energy for an infinite number of modes for $l_t/4\pi\, r \ll 1$:

$$\sum_{-\infty}^{\infty} F(m_0, l_t, r) = 1\,. \qquad (3)$$

According to Fig.2 a small transversal correlation length results in a large number of significantly excited aerodynamic modes, whereas a large l_t leads to a modal spectrum with a lower number of relevant modes. Herewith, the actually required cross-spectrum for the aerodynamic excitation can be modelled by the use of an auto-spectrum, forming the second part of Eq.(1). For the present study, the model assumed by Amiet [5] for the transversal correlation length is replaced by the Efimtsov model recently recalibrated by Haxter and Spehr [17] (see later Eq.(8)). To resolve the conflict in modelling an anisotropic problem with isotropic models, the prior used von Kármán turbulence spectrum for $S_{\theta\theta}(f)$ is substituted by the anisotropic Kerschen-Gliebe spectra [6, 16].

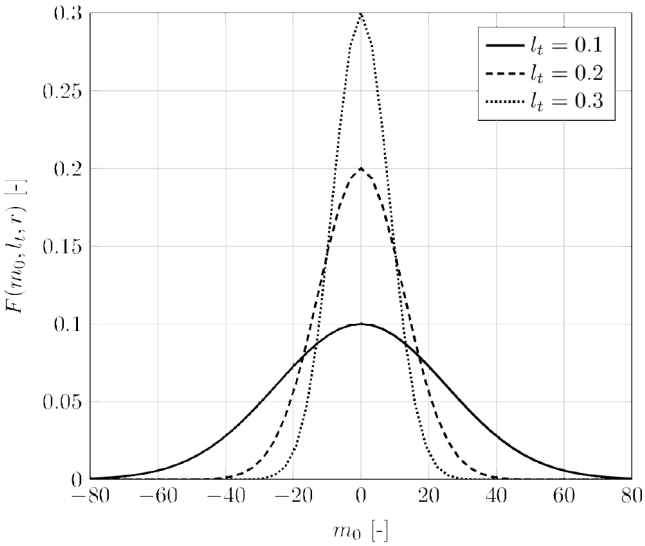

Fig.2: Exemplary Gaussian shaped coherence function F.

Acoustic radiation model

The second mechanism that has to be considered is the chopping of the same coherent structure by several consecutive rotor blades. According to Moreau [15] and Staggat et al. [16] the squared modal pressure for small l_t is given by:

$$|p_m|^2 = \Sigma(m) \int_r |G_m|^2 \cdot \overline{|\sigma|^2} \cdot l_t \, \mathrm{d}r\,, \qquad (4)$$

with the free-field Green's function G_m and an acoustic source term σ. The blade-to-blade correlation is accounted for by the modal weighting function $\Sigma(m)$ for the acoustic modes m, first defined by Moreau and Oertwig [19]:

$$\Sigma(m) = \sum_{\nu=1}^{B} \sum_{\nu'}^{B} \cos\left(2\pi \frac{m-m_0}{B}(\nu-\nu')\right) \exp\left(-\pi \left(\frac{s}{l_B}\right)^2 (\nu-\nu')^2\right). \qquad (5)$$

The steering parameter of the blade-to-blade correlation is the ratio of the blade spacing s to the blade correlation length l_B. Results for different ratios are plotted in Fig.3. If the ratio is close to one or larger than one, the blade-to-blade correlation of consecutive rotor blades is small and many acoustic modes are excited. If s is small (e.g. near the hub) or l_B becomes large (e.g. at high RPM) the interaction modes verifying $m = m_0 + kB$ are dominantly excited. For the limit of an infinite l_B only these interaction modes would be excited. The blade correlation length is given by [16]:

$$l_B = \sqrt{l_t^2 + \left(2\pi \, \frac{f_{rot} r}{U_{ref}} l_x\right)^2}, \qquad (6)$$

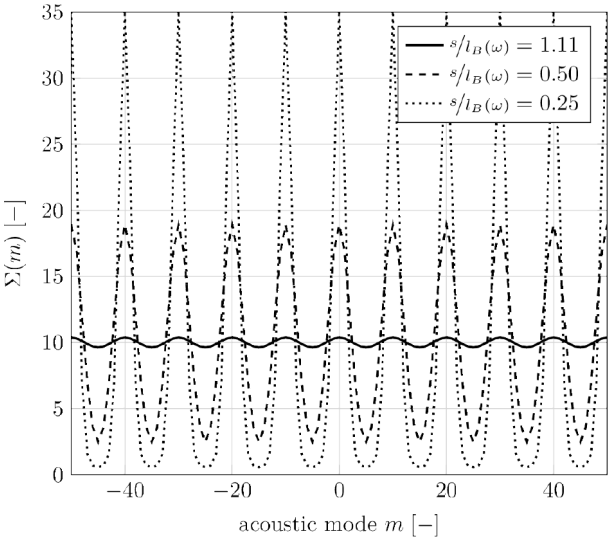

Fig.3: Modal weighting function $\Sigma(m)$ for 10 rotor blades

with f_{rot} the rotational frequency of the rotor, r the radial position and U_{ref} the velocity of the free stream. In the next subsection, the used models for the transversal and longitudinal correlation lengths l_t and l_x, as well as the implementation of the stream tube contraction required to model the functions $G(m_0, l_t, r)$, l_B and $\Sigma(m)$ are presented in more detail.

Model for the correlation length scales

In the past formulation of the theory, a prediction for the transversal correlation length l_t deduced from the isotropic von Kármán turbulence model by Amiet [5] was used. Amiet's assumption is valid for the mid- and high-frequency range but tends to zero for small frequencies. The small transversal correlation length in the low-frequency range contributed to distribute the energy across very high mode orders. Since only a limited amount of modes can numerically be taken into account, the truncation of the modal spectrum led to unphysical energy dissipation. This resulted in the occurrence of notches close to the BPF and its harmonics [16], because of the transformation into the rotating frame of reference, where the excitation of the acoustic sources has to be evaluated. That transformation is given by:

$$f_1 = f_0 + m_0 \cdot f_{rot} \,. \tag{7}$$

The longitudinal correlation length was originally estimated by a multiplication of the transversal correlation length with a factor of five hundred. This ad-hoc assumption was purely motivated by the observations of Hanson [18], who showed that the longitudinal extent of ingested coherent structures may reach several hundred times the transversal extent. Results for the correlation lengths l_x and l_t based on Amiet's assumption and Hanson's observation are shown as solid lines in Fig.4.

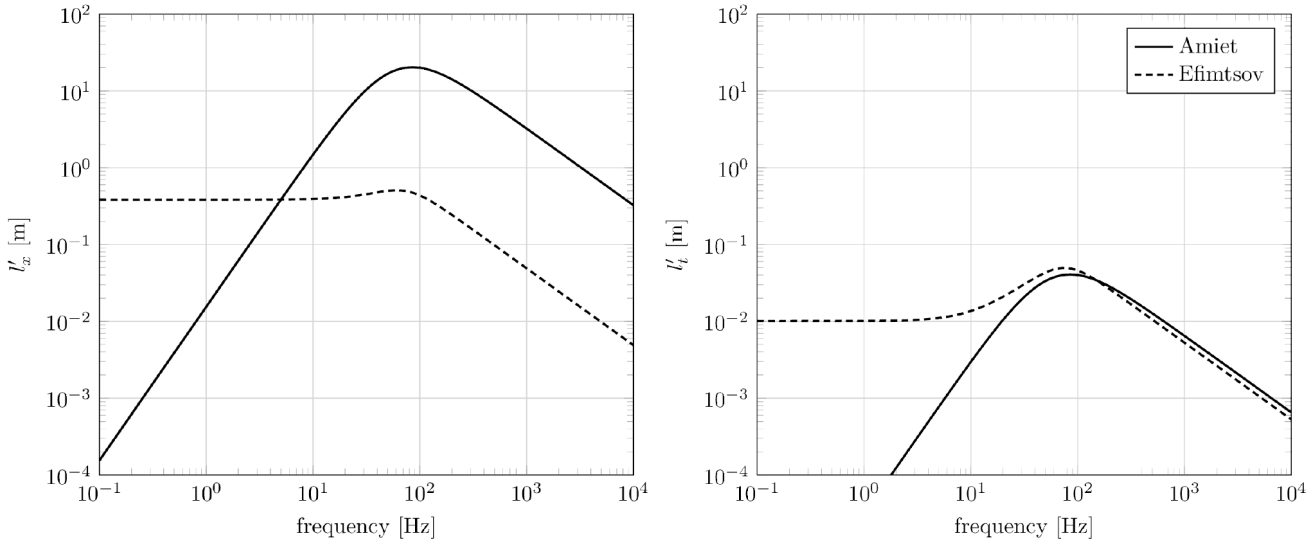

Fig.4: Comparison between the prior (Amiet) and currently (Efimtsov) models used to determine the longitudinal (left) and transversal (right) correlation lengths.

The problem of numerical dissipation for the low-frequency range and the ad-hoc assumption to estimate a longitudinal correlation length is solved by the use of an alternative model according to Haxter and Spehr [17]. This model is especially formulated for a turbulent boundary layer and a recalibration of earlier work of Efimtsov. It is based on recent experimental investigations on DLR A320 flight test carrier ATRA. The correlation lengths of this model are given by Eq.(8) [17]:

$$l'_{x/t}(St, u_c, u_\tau) = \delta_{99} \left(\left(\frac{a_{1/4}\, St}{u_c/u_\tau} \right)^2 + \frac{a_{2/5}^2}{St^2 + \left(a_{2/5}/a_{3/6}\right)^2} \right)^{-\frac{1}{2}} . \tag{8}$$

Note that the recalibrated constants $a_1 = 0.071$, $a_2 = 4.1$ and $a_3 = 0.26$ have to be used for the longitudinal correlation length. The prime indicates that the corresponding lengths are not yet the

final used correlation lengths which are affected by a stream tube contraction. The transversal correlation length is obtained by using the constants $a_4 = 0.66$, $a_5 = 39$ and $a_6 = 9.9$ in Eq.(8). For the current study, the friction velocity u_τ is computed based on the assumption of a logarithmic velocity profile with no adverse pressure gradient, adapted to the specifications of the benchmark (U_{ref} according to the operating point, kinematic viscosity ν, δ_{99} depending on U_{ref} and the von Kármán constant $\kappa = 0.38$). The convection velocity is given with $u_c = 0.75\, U_{ref}$. Finally the Strouhal number is defined as $St = 2\pi\, f\, \delta_{99}/u_\tau$.

Again, Fig.4 shows results for this modified Efimtsov model. It can be seen, that the transversal correlation length now tends towards a finite value in the low frequency range. The predicted lengths for the mid and high frequency range reveal a nearly identical result as the model assumed by Amiet. A second improvement results from the direct provision of a longitudinal correlation length l'_x by the model. Even though the longitudinal length is more than one magnitude larger than the transversal correlation length, it is significantly lower as when using Hanson's assumption.

Stream tube contraction

The fluid ingested by the rotor is accelerated and the fluid filaments and coherent structures are subject to a stream tube contraction. According to Ganz [12] a longitudinal contraction ratio c_l can be defined from the ratio of the velocities U_B after and U_A before the stream tube contraction:

$$c_l = U_B/U_A\,. \tag{9}$$

The stream tube contraction also leads to a shortening of the coherent structures in transversal directions. Following Ganz [12] the contraction in transversal direction is given by continuity:

$$c_t = \sqrt{\frac{\rho_{ref}}{\rho_B} \cdot \frac{1}{c_l}}\,. \tag{10}$$

Note that an equal contraction in both transversal directions is assumed to obtain Eq.(10). For the present study an incompressible flow is assumed. This is justified by the Mach number range $M \in [0.03, 0.09]$ of the benchmark. Thus, for Eq.(10) $\rho_{ref} = \rho_B$ holds. The correlation lengths l_x and l_t after stream tube contraction, used in this study for Eqs.(2), (4) and (6), are finally obtained by multiplication:

$$l_{l/t} = c_{l/t} \cdot l'_{l/t} \tag{11}$$

Based on blade element momentum and actuator disc theory according to Glauert [20], the post contraction velocity, caused by the rotor, can be described by the rotor propulsive efficiency η:

$$c_l = 1/\eta\,. \tag{12}$$

The propulsive efficiency of the benchmark rotor can be also estimated by using blade element momentum theory in an iterative procedure. Required input parameters are the blade chord length, tip and hub diameter, the blade stagger angles at hub and tip, blade count, rotational speed and density of air. The rotor design advance ratio is known with $J_{DP} = 1.17$ from Morton et al. [21]. Note that the advance ratio is defined by: $J = U_{ref}/(f_{rot}\, D)$. Estimations of the propulsive efficiency for the four investigated OPs are shown in Fig.5. It should be noted that the presented efficiency estimation contains uncertainties with regard to the input parameters: the stagger angle is assumed to linearly vary over the span, which is not the case in reality. In addition the used blade element method neglects three-dimensional flow velocities induced by the rotor, the tip vortex and radial flow components.

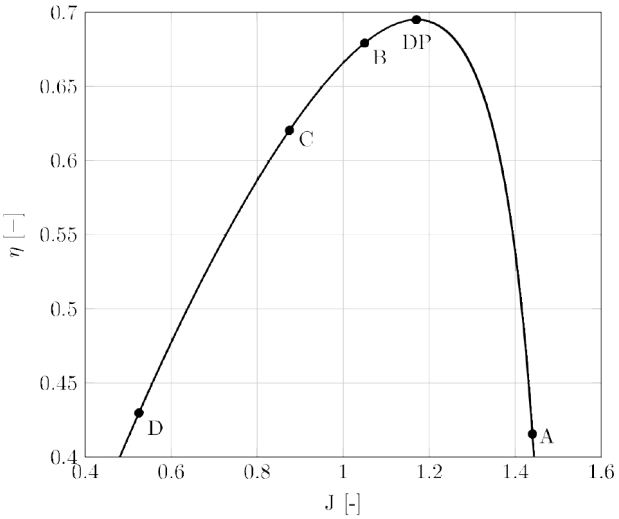

Fig. 5: Estimated efficiency of FC3 rotor based on actuator disc theory for design (DP) and investigated operating points A, B, C and D.

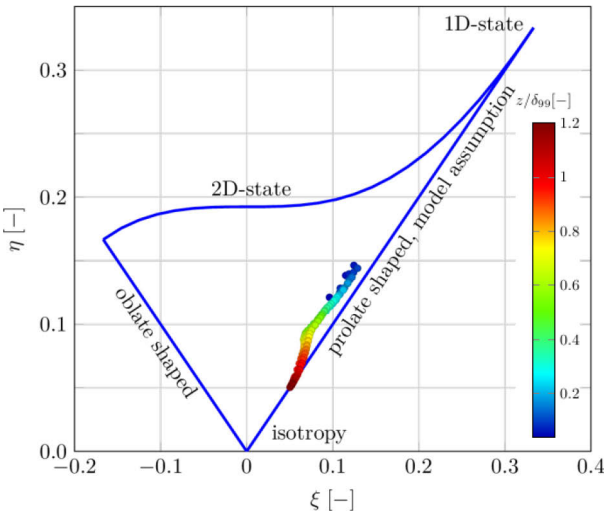

Fig. 6: Classification of the measured benchmark turbulence within the turbulence triangle.

APPLICATION

The presented theory is now applied to the experimental benchmark case so-called *"FC3"* defined within the framework of the *"Fan Broadband Noise Prediction workshop"* hosted by the AIAA organisation [22]. The experimental set-up is shown in Fig.7: an open rotor with 10 blades is mounted at one wall of the wind tunnel in such a way that a tip clearance of approximately 6% of blade span is ensured between the wall and the rotating blades. In addition a planar boundary layer is developing at the wall on which the rotor is mounted. A trip, mounted 4.76 m upstream of the rotor plane ensures that this boundary layer is turbulent when reaching the rotor. For the presented operating points a boundary layer thickness δ_{99} of about 0.10 m was measured at the rotor face, which means that only 25% of the rotor blade span is embedded in the boundary layer. Since the presented theory assumes axisymmetric turbulence the question arise, if this state of turbulence is found in the present application of an open rotor ingesting a turbulent boundary layer. Figure 6 shows a classification of the benchmark turbulence as specified by Choi and Lumley [23] for several positions normal to the wall. The figure indeed reveals a trend of the turbulence towards axisymmetric and prolate shaped turbulence for locations within the turbulent boundary layer. This state is ideally achieved for points on the right leg of the triangle. Note that the presented theory assumes a state of turbulence which rather coincides with the upper right leg region of the turbulence triangle.

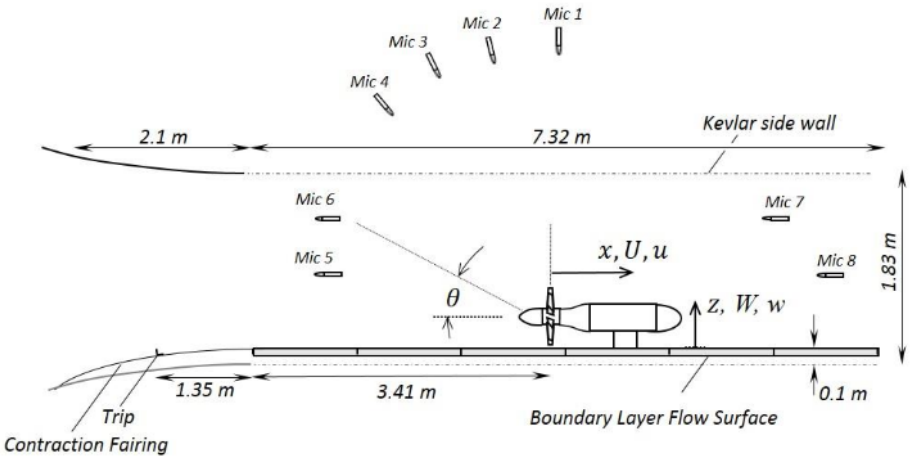

Fig.7: Illustration of the FC3 benchmark.
Sketch reproduced with permission from benchmark program publication [22].

A detailed description of the test rig, the measurements and the properties of the turbulent flow field is given in [21, 24 and 25].

The provided data contains the mean flow profiles in x, y and z direction as well as the test conditions such as the static density of air and the sound speed. The unsteady properties of the boundary layer are provided by a correlation tensor of the form $R_{ij}(z, z', \Delta y, dt)$. The workshop data is sampled at a plane approximately 0.04 m upstream of the rotor leading edges in absence of the rotor. The extent of this plane is about: $y \in [0, 1.18]/\delta_{99}$ and $z/z' \in [0.04,\ 1.22]/\delta_{99}$ according to the coordinate system shown in Fig.1. The range of time delay is $dt \in [-5, 5] \cdot U_{ref}/\delta_{99}$. For the present study only the auto-correlation $R_{ii}(z, z, 0, dt)$ of the turbulent velocity fluctuations is evaluated. The obtained auto-correlations are transformed to auto-spectra $\Phi_{ii}(z, z, 0, f)$ by Fourier transformation. The turbulent velocity spectra for different locations z within the turbulent boundary layer are extended laterally in y-direction in such a way that a coverage of the whole rotor diameter is ensured. Hereby the same auto-spectra are assumed for each y-position. For the positions outside of the boundary layer ($z > \delta_{99}$) the auto-spectra are assumed to be zero. The Cartesian representations of the auto-spectra are interpolated to polar coordinates. Finally the spectra are averaged in the circumferential direction. Note that the longitudinal spectrum $\Phi_x(f, r)$ is given by $\Phi_{uu}(f, r)$ and the transversal spectra $\Phi_{vv}(f, r)$ and $\Phi_{ww}(f, r)$ are summed to a total transversal spectrum $\Phi_t(f, r)$. The spectra are fitted to one-dimensional Kerschen-Gliebe spectra for anisotropic axisymmetric turbulence. The one-dimensional spectra can be obtained by integration of the two-dimensional spectra defined in [6]. The equations read:

$$\Phi_x(f) = \frac{2\,u_x^2 \Lambda_x}{U_{ref}} \cdot \frac{1}{1+\left(\frac{2\pi f}{U_{ref}} \cdot \Lambda_x\right)^2}, \tag{13}$$

$$\Phi_t(f) = \frac{u_x^2 \Lambda_x}{U_{ref}} \cdot \frac{1}{1+\left(\frac{2\pi f}{U_{ref}} \cdot \Lambda_x\right)^2} \cdot \left(2\left(\frac{u_t}{u_x}\right)^2 - \left(\frac{\Lambda_t}{\Lambda_x}\right)^2 + 2 \cdot \left(\frac{2\pi f}{U_{ref}} \cdot \Lambda_t\right)^2 \cdot \frac{1}{1+\left(\frac{2\pi f}{U_{ref}} \cdot \Lambda_x\right)^2} \right). \tag{14}$$

with u_x and u_t the turbulent velocities in longitudinal and transversal direction, Λ_x and Λ_t the scalar longitudinal and transversal turbulent length scales and U_{ref} the reference velocity to transform the spectra from the wavenumber into the frequency domain. In the fitting process the longitudinal spectrum is fitted first to determine u_x and Λ_x. In a second step, the transversal spectrum is fitted and the remaining parameters u_t and Λ_t are obtained. Finally, the total spectrum $\Phi_{turb} = \Phi_x + \Phi_t$ is used as input for $S_{\theta\theta}(f)$ in Eq.(1). It should be noted at this point that the scalar correlation length scales and the spectra of the correlation lengths are decoupled from each other in the present model, although we may expect some physical dependency between them.

Table 1: Summary of operating conditions and estimated propulsive efficiency.

Case	U_{ref} [m/s]	RPM [min^{-1}]	J [-]	Est. η [-]
A	30.0	2734	1.44	0.42
B	20.0	2500	1.05	0.68
C	30.0	4500	0.87	0.62
D	10.0	2500	0.52	0.43

In total four OPs at low and high thrust conditions are evaluated. Only results for microphone number 5 according to Fig.7 are shown. It must be noted, that the wind tunnel plate is considered as an absorbing wall. Thus, effects caused by a reflection of the sound at the hard wall (e.g.

interferences) are not captured by the presented model. The OPs are defined according to Tab.1 by their advance ratios J. Figure 8 compares predicted sound pressure level (SPL) of the improved theory (theory$_{17}$) to the old theory (theory$_{15}$) presented in Staggat et al. [16]. The large discrepancy of more than 20 dB observed in the past compared to the measurement is clearly reduced with the new approach. This mostly results from the direct fit of the Kerschen-Gliebe spectra with the spectra obtained from the auto-correlation tensor R_{ii} that provides the length scales $\Lambda_{x/t}$ and turbulent velocities $u_{x/t}$. In the past study, these velocities were obtained from the azimuthal averaged turbulent velocity profiles. A good agreement between measurement and prediction is obtained at the BPF for OPs A, B and C. The second harmonic is captured with a fair agreement too. For high loading conditions (Case D) the theory clearly under predicts the noise at the first, second and third BPF by more than 10 dB. For this OP a boundary layer – vortex interaction was identified in the measurements by Wisda et al. [26] and it was shown by Glegg et al. [27, 28] that this additional noise source contributes significantly to the SPL at the BPF and its higher harmonics. For the frequency band between the BPF humps and its harmonics the presented theory tends to over predict the SPL by approximately 10 dB (Case A,B,C).

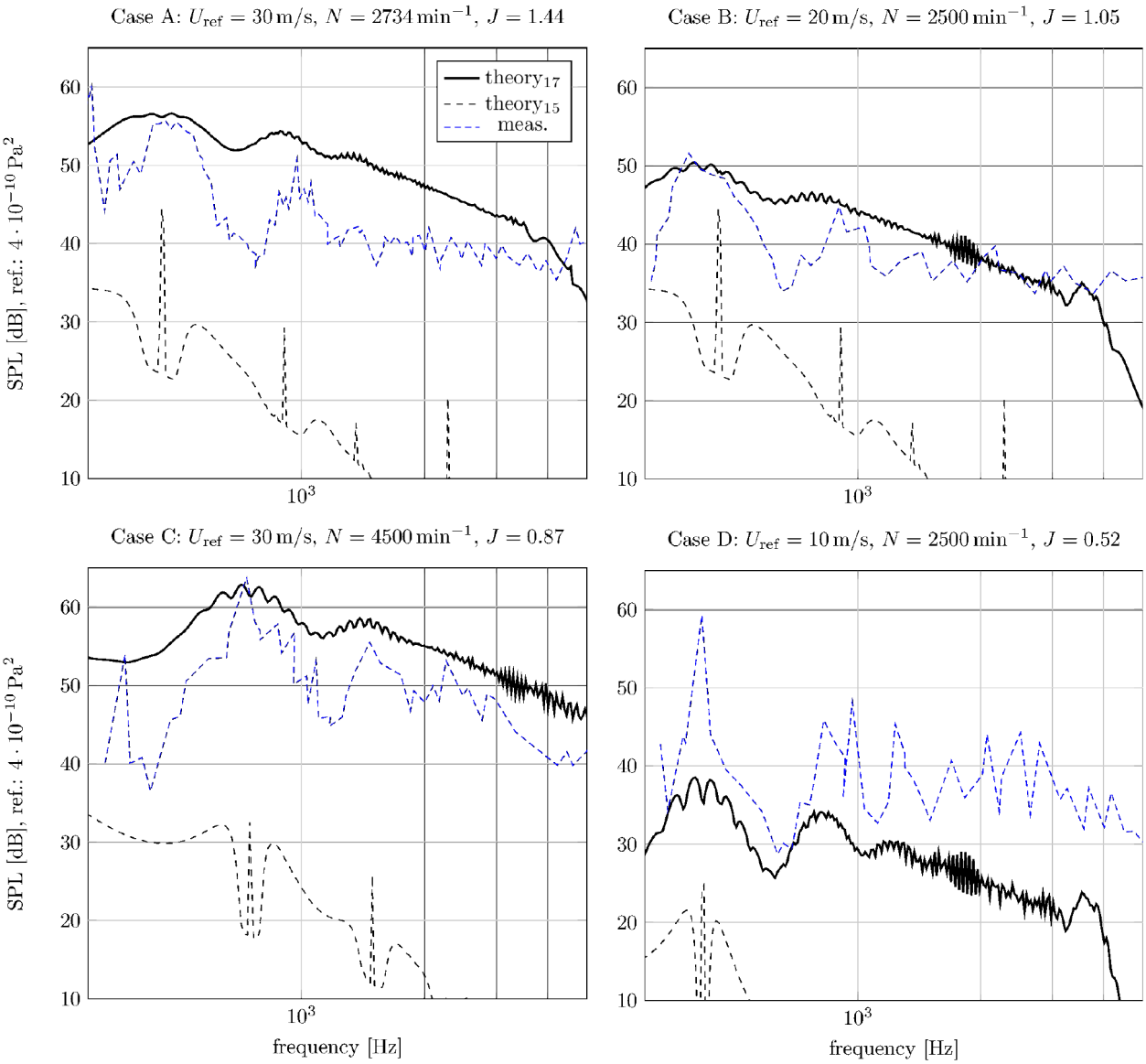

Fig.8: Comparison of predicted SPL and measurement for different advance ratios J. Observer angle: 14.4°, observer distance: 2.24 m (according to Mic.5 in Fig. 7). Measurement data reproduced with permission.

Another improvement is the absence of the sharp notches left and right of the BPF and its harmonics. Note that the dissipation due to truncation also occurs at higher frequencies in the improved theory since the number of circumferential modes is limited by numerical reasons and the correlation lengths of the recalibrated Efimtsov model are nearly identical to the lengths predicted by the model of Amiet.

The widening and narrowing of the BPF-centred bumps dependent on the OP, already observed in the original model, is also reproduced by the improved theory in accordance to the measurements. The smaller peaks in the predicted BBN spectrum with its larger bumps centred at the BPF and its harmonics occur at engine orders (EO) and result from the distribution of the energy across the circumferential modes. It should be noted, that this spectral feature is sensitive to the longitudinal correlation length l_x and is therefore strongly dependent on the estimation of the stream tube contraction.

CONCLUSION

An analytical theory for the prediction of the interaction noise of a turbulent boundary layer with a rotor was presented. The theory assumes anisotropic axisymmetric turbulence to reproduce the existence of large coherent structures in the turbulent boundary layer. This work addresses problems identified by Staggat et al. [16] in a first formulation of the theory that largely used the approach proposed by Amiet [4, 15] for the modelling of turbulence-airfoil interaction noise. The small extent of the boundary-layer coherent structures in transversal direction leads to an aerodynamic excitation spectrum containing high aerodynamic mode orders. The large extent of those structures in longitudinal direction leads to a correlation of the sound field between consecutive rotor blades and a preferred excitation of interaction modes that radiate at the BPF and its higher harmonics.

The present work improves central components of Amiet's theory: in contrast to the isotropic von Kármán spectrum, the now used Kerschen-Gliebe spectra reflect the spectral properties of anisotropic axisymmetric turbulence as encountered in boundary layers by a different integral length scale for the longitudinal and transversal direction but also two different levels of turbulent kinetic energy. The direct fitting of the spectra with experimental data mostly explains the much better agreement of the predicted sound pressure levels with the measurements. The prior used correlation length model assumed by Amiet is replaced by a model proposed by Haxter & Spehr [17] especially developed for turbulent boundary layers. The advantage of this model is twofold: i) the ad-hoc assumption to estimate the longitudinal correlation length l_x can be replaced by a physically motivated model; ii) the non-zero and in principle constant value for the transversal correlation length l_t predicted in the low-frequency range avoids the numerical energy dissipation resulting in non-physical notches beside the BPF frequencies. Finally, the elongation and contraction of the longitudinal and transversal correlation lengths due to the rotor thrust has been included in the modelling via the stream tube contraction of the mean flow, which is estimated from the actuator disc theory by the propulsive efficiency. The consideration of stream tube contraction becomes necessary since the correlation lengths provided by the modified Efimtsov model do not include the effect of the rotor on the stream. In particular the predicted longitudinal correlation length l_l' is too small to reveal the observed peaks centred at the BPF and its harmonics. The shortening effect on the transversal correlation length l_t' is included but can be considered as secondary. Thus, in accordance to Majumdar and Peake [13] the stream tube contraction seems to be a relevant dynamic process that has to be incorporated for boundary layer interaction noise based on the here assumed phenomenology. Note that considering the stream tube contraction seemed unnecessary in Staggat et al. [16], since the used ad-hoc assumption for l_x predicted a sufficient large correlation length that reveals bumps at the BPF and its harmonics.

A comparison of the original and improved theory yields a much better agreement of the SPL as well as the spectral shape with measurement data for four different operating points with different thrust conditions.

ACKNOWLEDGMENT

The project leading to this application has received funding from the Clean Sky 2 Joint Undertaking under the European Union's Horizon 2020 research and innovation programme under Grant Agreement No. CS2-GAM-2016-2017-LPA.

The authors would like to thank John Coupland, University of Southampton, for coordinating the "Fan Broadband Noise Prediction Workshop", as well as William Devenport and Nathan Alexander, Virginia Tech, for providing the experimental data of the test case.

BIBLIOGRAPHY

[1] R. Liebeck – *Design of the Blended Wing Body Subsonic Transport.* Journal of Aircraft, Vol.41, No.1, pp.10-25, **2004**

[2] R. Mani – *NOISE DUE TO INTERACTION OF INLET TURBULENCE WITH ISOLATED STATORS AND ROTORS.* Journal of Sound and Vibration, Vol.17, No.2, pp.251-260, **1971**

[3] G.F. Homicz, A.R. George – *Broadband and discrete frequency radiation from subsonic rotors*. Journal of Sound and Vibration, Vol.36, No.2, pp.151-177, **1974**

[4] R. Amiet – *ACOUSTIC RADIATION FROM AN AIRFOIL IN A TURBULENT STREAM.* Journal of Sound and Vibration, Vol.41, No.4, pp.407-420, **1975**

[5] R.W. Paterson, R.K. Amiet – *Noise of a Model Helicopter Rotor Due to Ingestion of Turbulence.* NASA Contractor Report 3213, **1979**

[6] E.J. Kerschen, P.R. Gliebe – *Noise Caused by the Interaction of a Rotor with Anisotropic Turbulence.* AIAA Journal, Vol.19, No.6, pp.717-723, **1981**

[7] S. Glegg, N. Walker – *FAN NOISE FROM BLADES MOVING THROUGH BOUNDARY LAYER TURBULENCE.* 5th AIAA/CEAS Aeroacoustics Conference, Bellevue (WA, USA), **1999**, AIAA-99-1888

[8] S. Glegg – *THE RESPONSE OF A SWEPT BLADE ROW TO A THREE-DIMENSIONAL GUST.* Journal of Sound and Vibration, Vol.227, No.1, pp.29-64, **1998**

[9] S. Glegg, M. Morton, W. Devenport – *Rotor Inflow Noise Caused by a Boundary Layer: Theory and Examples.* 18th AIAA/CEAS Aeroacoustics Conference, Colorado Springs (CO, USA), **2012**, AIAA-2012-2263

[10] D. Stephens, S. Morris – *Sound Generation by a Rotor Interacting with a Casing Turbulent Boundary Layer.* AIAA Journal, Vol.47, No.11, pp.2698-2708, **2009**

[11] S. Glegg, W. Devenport, N. Alexander – *Broadband rotor noise predictions using a time domain approach.* Journal of Sound and Vibration, Vol.335, pp.115-124, **2013**

[12] U. Ganz – *Analytical Investigation of Fan tone Noise Due to Ingested Atmospheric Turbulence.* NASA Contractor Report 3302, **1980**, NAS1-15085

[13] S. Majumdar, N. Peak – *Noise generation by the interaction between ingested turbulence and a rotating fan.* Journal of Fluid Mechanics, Vol.359, pp.180-216, **1998**

[14] H. Atassi, M. Logue – *Fan Broadband Noise in Anisotropic Turbulence.* 15th AIAA/CEAS Aeroacoustics Conference, Miami (FL, USA), **2009**, AIAA-2009-3148

[15] A. Moreau – *A unified analytical approach for the acoustic conceptual design of fans of modern aero-engines.* PhD Thesis, Technical University of Berlin, Berlin (Germany), **2017**

[16] M. Staggat, A. Moreau, S. Guérin – *Boundary Layer Induced Rotor Noise Using an Analytical Modal Approach*. 22nd AIAA/CEAS Aeroacoustics Conference, Lyon (France), **2016**, AIAA-2016-2997

[17] S. Haxter, C. Spehr – *Comparison of model predictions for coherence length to in-flight measurements at cruise conditions.* Journal of Sound and Vibration, Vol.390, pp.86-117, **2017**

[18] D. Hanson – *Spectrum of rotor noise caused by atmospheric turbulence*. The Journal of the Acoustical Society of America, Vol.56, No.1, pp.110-126, **1974**

[19] A. Moreau, S. Oertwig – *Measurements compared to analytical prediction of the sound emitted by a high-speed fan stage.* 19th AIAA/CEAS Aeroacoustics Conference, Berlin (Germany), **2013**, AIAA-2013-2047

[20] H. Glauert – *The Elements of aerofoil and airscrew theory*, Cambridge University Press, **1943**

[21] M. Morton, W. Devenport, W.N. Alexander – *Rotor Inflow Noise Caused by a Boundary Layer: Inflow Measurements and Noise Predictions.* 18th AIAA/CEAS Aeroacoustics Conference, Colorado Springs (CO, USA), **2012**, AIAA-2012-2120

[22] http://www.oai.org/aeroacoustics/docs/FC3_Specification_Version1.pdf (visited: 2018-02-06)

[23] K. Choi, J.L. Lumley – *The return to isotropy of homogeneous turbulence.* Journal of Fluid Mechanics, Vol.436, pp.59-84, **2001**

[24] W.N. Alexander, W. Devenport, D. Wisda, M. Morton, S. Glegg – *Sound Radiated From a Rotor and Its Relation to Rotating Frame Measurements of Ingested Turbulence.* 20th AIAA/CEAS Aeroacoustics Conference, Atlanta (GA, USA), **2014**, AIAA-2014-2746

[25] D. Wisda, W. Alexander, W. Devenport, S. Glegg, A. Borgoltz – *Boundary Layer Ingestion Noise and Turbulence Scale Analysis at High and Low Advance Ratios.* 20th AIAA/CEAS Aeroacoustics Conference, Atlanta (GA, USA), **2014**, AIAA-2014-2608

[26] D. Wisda, H. Murray, W. Alexander, M. Nelson, W. Devenport, S. Glegg – *Flow Distortion and Noise Produced by a Thrusting Rotor Ingesting a Planar Turbulent Boundary Layer*. 21st AIAA/CEAS Aeroacoustics Conference, Dallas (TX, USA), **2015**, AIAA-2015-2981

[27] S. Glegg, A. Buono, J. Grant, F. Lachowski – *Sound Radiation from a Rotor Partially Immersed in a Turbulent Boundary Layer*, 21st AIAA/CEAS Aeroacoustics Conference, Dallas (TX, USA), **2015**, AIAA-2015-2361

[28] S. Glegg, J. Grant, H. Murray, W. Devenport, N. Alexander – *Sound Radiated from a Rotor Operating at High Thrust Near a Wall*, 22nd AIAA/CEAS Aeroacoustics Conference, Lyon (France), **2016**, AIAA-2016-2995